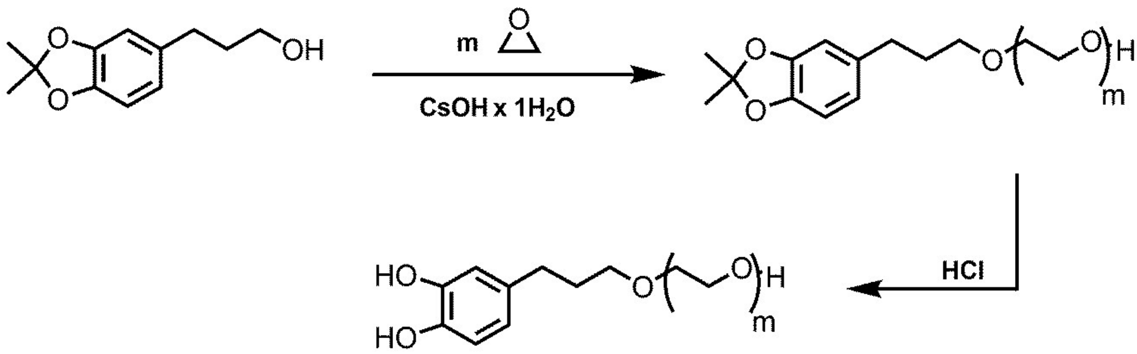

Scheme S1. Synthesis scheme of catechol-PEG: Polymerization of ethylene oxide (EO), followed by deprotection of CA-PEG with an aqueous solution of hydrochloric acid resulting in hydrophilic C-PEG.

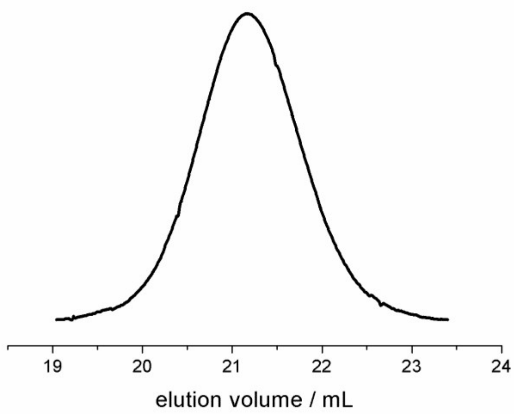

Composition$_{NMR}$	$M_{n,NMR}$[a] / g· mol^{-1}	$M_{n,GPC}$[b] / g· mol^{-1}	$M_{w,GPC}$[b] / g· mol^{-1}	M_w/M_n[b]
CA-PEG$_{67}$	3160	2450	2610	1.07

[a]Calculated from ^{1}H-NMR spectrum. [b]Determined by GPC in DMF (RI, PEG standard).

Figure S1. GPC trace (RI, DMF, PEG standard) of CA-PEG$_{67}$.

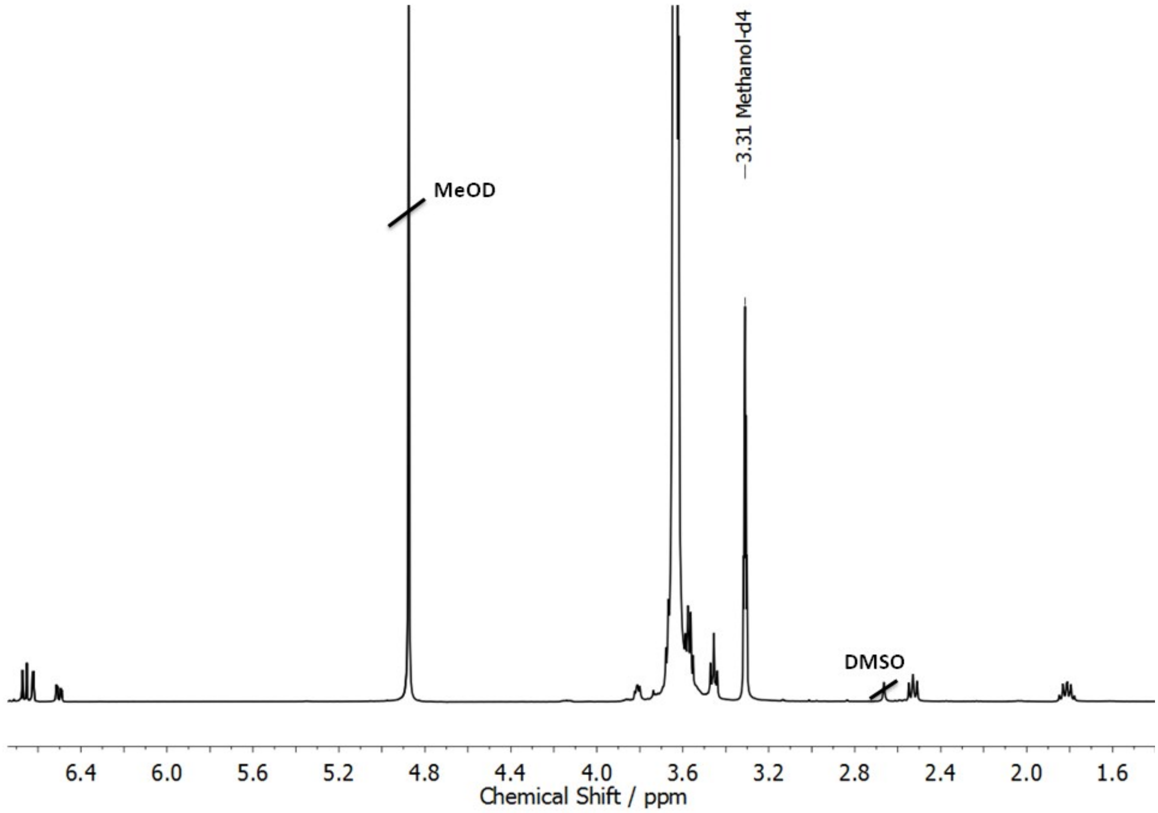

Figure S2. ^{1}H NMR spectrum (400 MHz, methanol-d_4) of catechol-PEG (C-PEG_{67}) after release of the protecting groups.

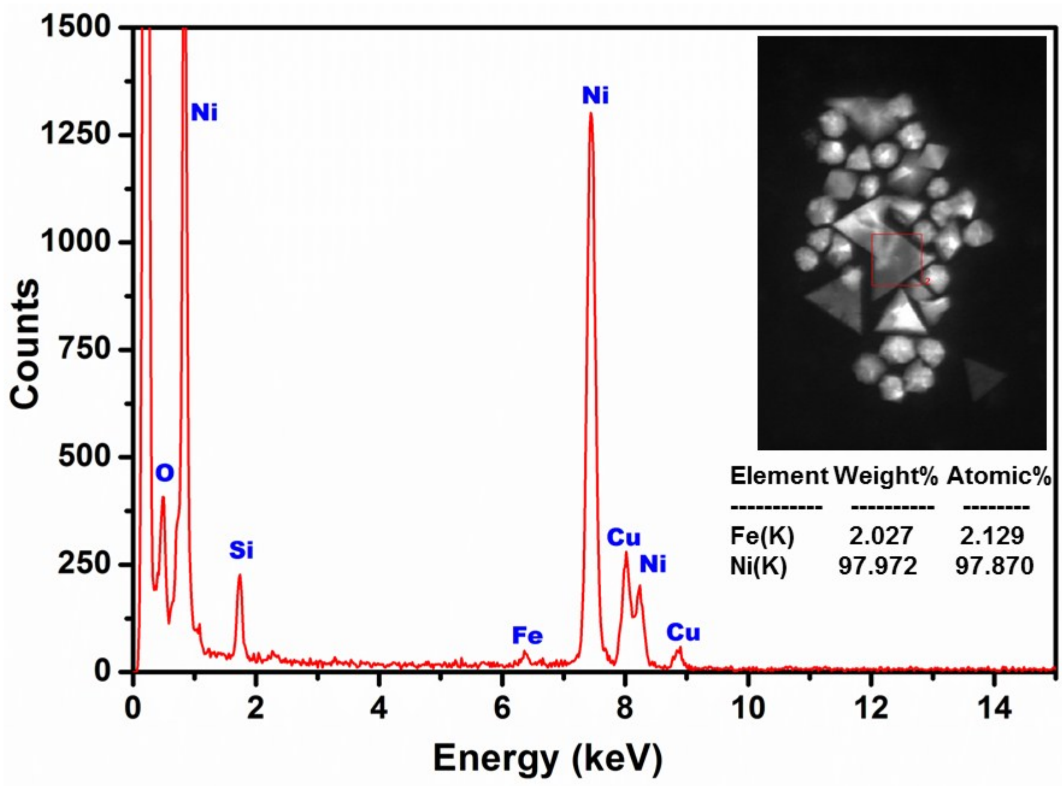

Figure S3. EDX spectrum from $Ni_{0.95}Fe_{0.05}$ precursors after a reaction time of 6 minutes.

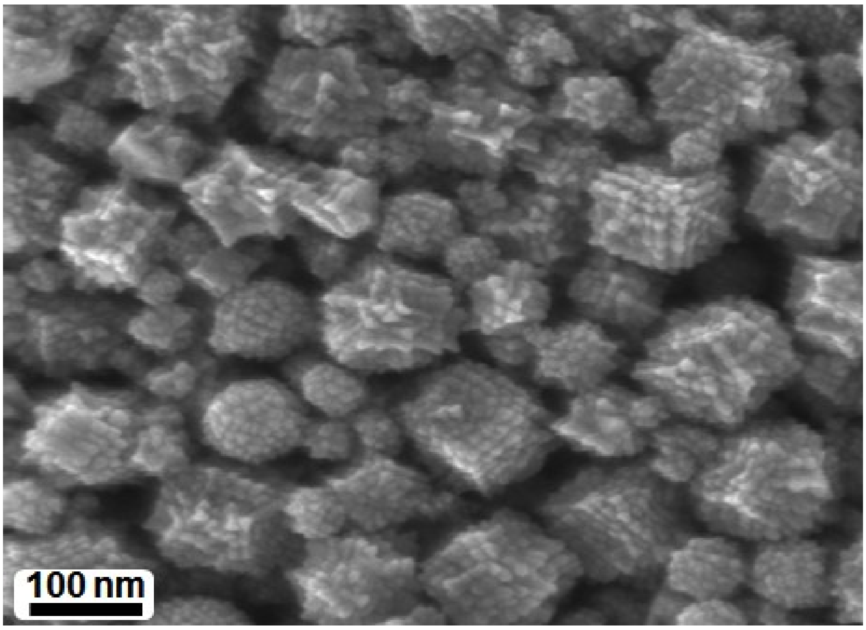

Fig. S4: An SEM image to confirm a better overview and hierarchical arrangements of nanodomains in three dimensional (3D) patterns

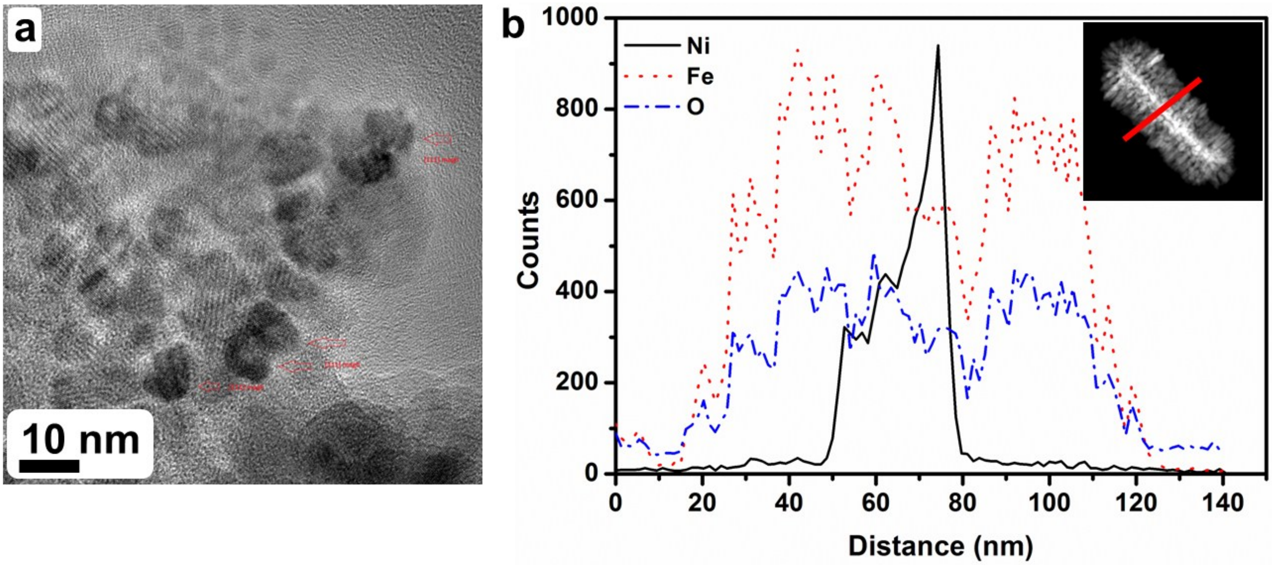

Figure S5. (**a**) HRTEM of a superparticle showing that all the rods growing on the flat surface have the same orientation, with [111] as the main direction of growth (**b**) z-contrast image (STEM) of a plate standing on the short side (inset) and corresponding line scan elemental analysis to confirm hierarchically organized iron oxide around nickel nanoplates.

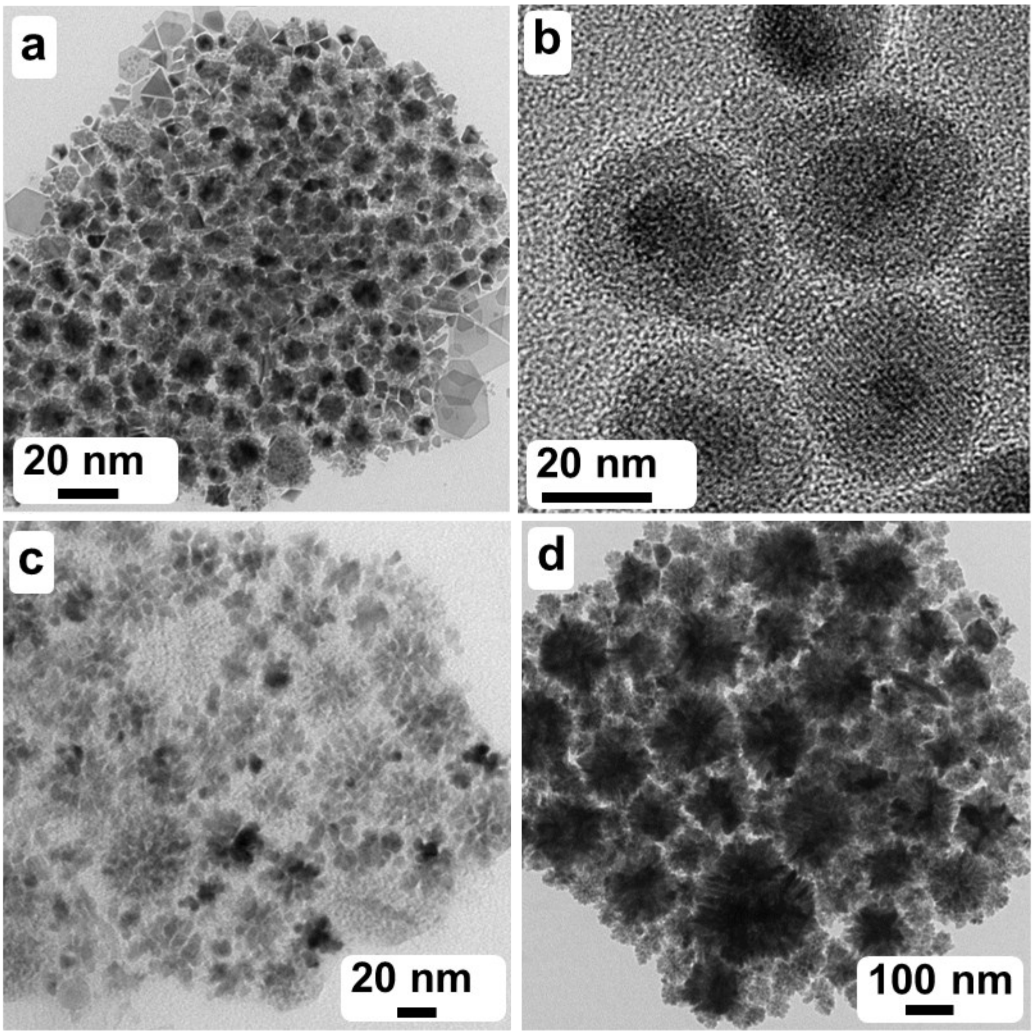

Figure S6. TEM images of (**a**) $Ni_{0.95}$ $Fe_{0.05}$@γ-Fe_2O_3 nanoparticles when $Fe(CO)_5$ was injected at 180 °C (**b**) at 240 °C and varying the amount of injected $Fe(CO)_5$, 10 μL (**c**) and 200 10 μL (**d**).

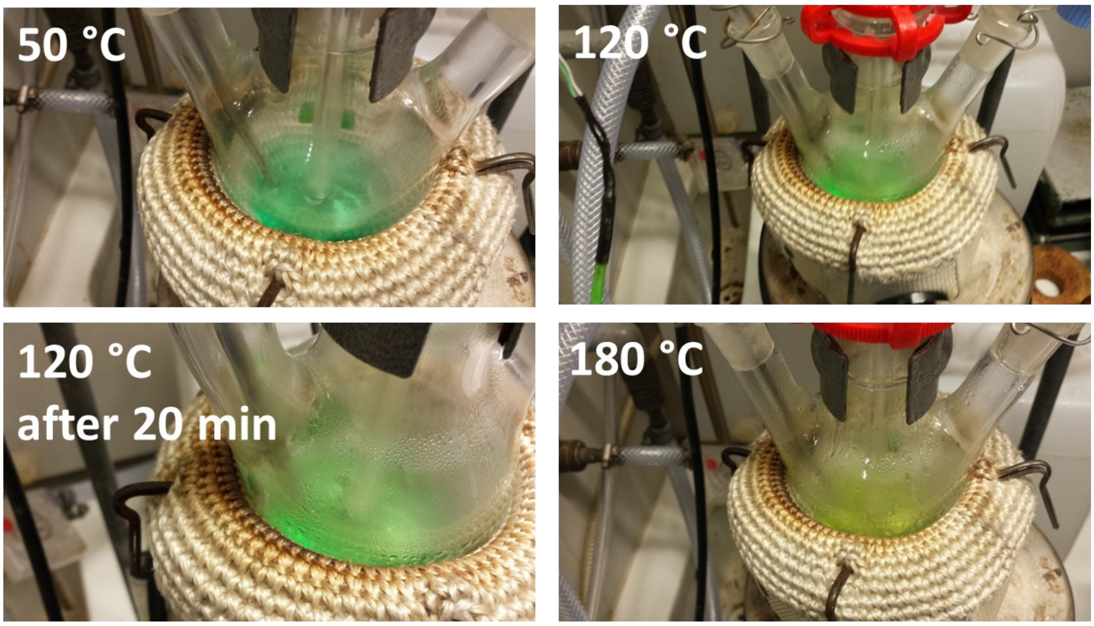

Figure S7. Digital camera photograph of reaction flask at various temperatures in the absence of $Fe(CO)_5$.

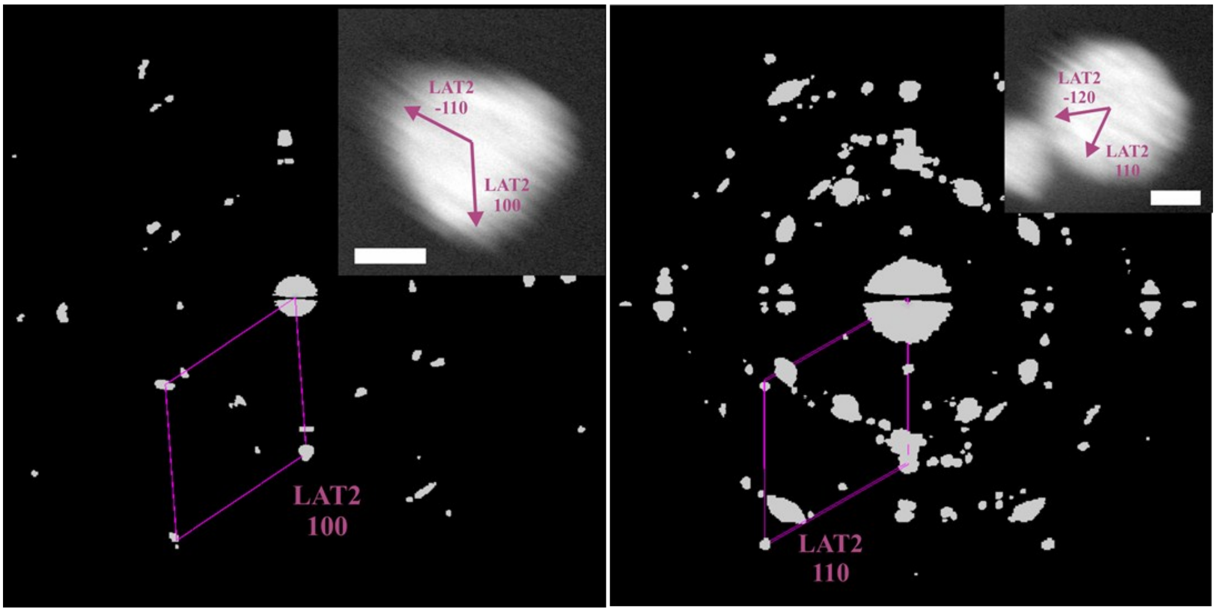

Figure S8. Orientation of LAT2 (in violet) in relation with the (**a**) triangular and (**b**) hexagonal shaped superparticles. Images were taken in STEM μ-probe mode with an extremely reduced illumination. Three-dimensional diffraction reconstructions were performed by ADT. Scale bar: 100 nm.

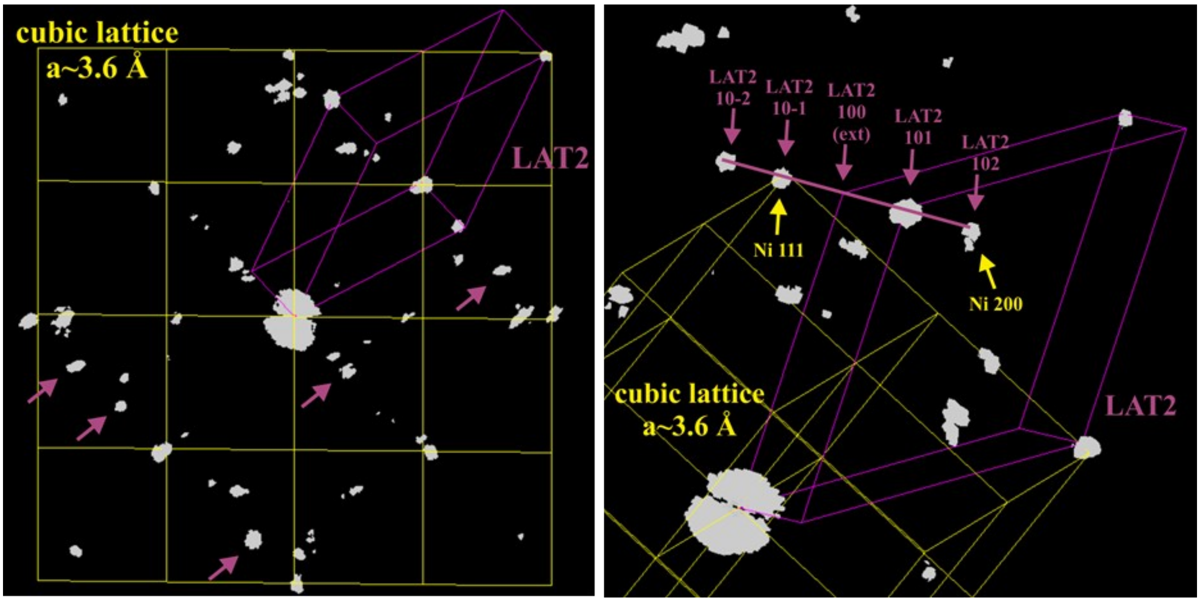

Figure S9. Geometrical relations between hexagonal LAT2 (in violet) and the commensurate cubic cell with a~3.6 Å (in yellow) determined by P-XRP and reported in literature for □-metals and permalloys. (**a**) View along (100)* of the cubic cell, with LAT2 extra-reflections indicated by violet arrows. (**b**) Reciprocal lattice section showing the extra-reflections close to the 111 reflection of cubic Ni. Three-dimensional diffraction reconstructions were performed by ADT.

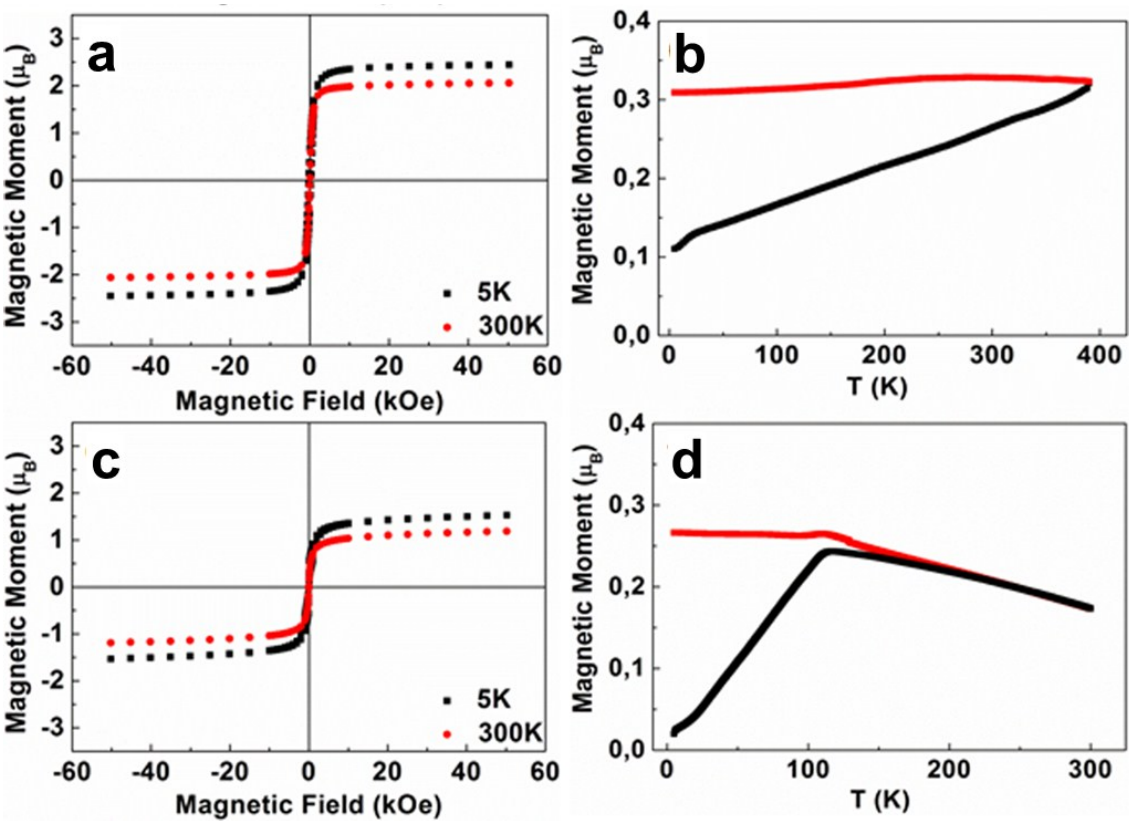

Figure S10. Magnetic properties of the Ni@γ-Fe_2O_3 core shell nanoparticles. Magnetic hysteresis loops at 5 K and 300 K and temperature dependence of the magnetization in field-cooling (FC) and zero-field-cooling (ZFC) of Ni@γ-Fe_2O_3 heterodimer nanoparticles (a,b) and core-shell nanoparticles (c,d) respectively.